

Article

# Behavior of Calcium Compounds under Hydrothermal Conditions during Alkaline Leaching of Aluminosilicates with the Synthesis of Fillers for Composites

Rinat Abdulvaliyev <sup>1</sup>, Nazym Akhmediyeva <sup>1,\*</sup>, Sergey Gladyshev <sup>1</sup>, Nazira Samenova <sup>1</sup>,  
Olga Kolesnikova <sup>2,\*</sup> and Olimpiada Mankesheva <sup>3</sup>

<sup>1</sup> Institute of Metallurgy and Ore Beneficiation, Satbayev University, Almaty 050010, Kazakhstan; rin-abd@mail.ru (R.A.); gladyshev.sergey55@mail.ru (S.G.); nazira.orakkyzy@gmail.com (N.S.)

<sup>2</sup> Department of Science, Production and Innovation, M. Auezov South Kazakhstan University, Shymkent 160012, Kazakhstan

<sup>3</sup> Department of Maritime Academy, Sh. Yessenov Caspian University of Technology and Engineering, Aktau 130002, Kazakhstan; olimpiada.mankesheva@yu.edu.kz

\* Correspondence: n.akhmediyeva@satbayev.university (N.A.); ogkolesnikova@yandex.kz (O.K.); Tel.: +7-707-190-01-14 (N.A.)

**Abstract:** Calcium oxide plays an important role in alumina production by binding SiO<sub>2</sub> from aluminosilicate raw materials (bauxite, nepheline, kaolinite, etc.) in aluminum-free compounds. The efficiency of the hydrochemical technology depends on the activities of calcium oxide or its compounds introduced into the alkaline aluminosilicate slurry. In this paper, we considered the effects of different calcium compounds (calcium carbonate CaCO<sub>3</sub>, gypsum CaSO<sub>4</sub>·H<sub>2</sub>O, calcium oxide CaO and calcium hydroxide Ca(OH)<sub>2</sub>), introduced during the hydrothermal stripping of aluminosilicates with alkaline solutions, on the degree of aluminum oxide extraction, with the subsequent production of fillers for composites. Ca(OH)<sub>2</sub> was obtained by the CaO quenching method. Extraction of Al<sub>2</sub>O<sub>3</sub> in an alkaline solution was only possible with Ca(OH)<sub>2</sub>, and the degree of extraction depended on the conditions used for CaO quenching. The effects of temperature and of the duration of CaO quenching on particle size were investigated. In potassium solution, the best results for Al<sub>2</sub>O<sub>3</sub> extraction were obtained using CaSO<sub>4</sub>·H<sub>2</sub>O gypsum. The obtained solutions were processed using the crystallization method.

**Keywords:** aluminosilicate; calcium additive; silica; lime; lime quenching; composites



**Citation:** Abdulvaliyev, R.; Akhmediyeva, N.; Gladyshev, S.; Samenova, N.; Kolesnikova, O.; Mankesheva, O. Behavior of Calcium Compounds under Hydrothermal Conditions during Alkaline Leaching of Aluminosilicates with the Synthesis of Fillers for Composites. *J. Compos. Sci.* **2023**, *7*, 508. <https://doi.org/10.3390/jcs7120508>

Academic Editor: Francesco Tornabene

Received: 16 October 2023  
Revised: 7 November 2023  
Accepted: 1 December 2023  
Published: 5 December 2023



**Copyright:** © 2023 by the authors. Licensee MDPI, Basel, Switzerland. This article is an open access article distributed under the terms and conditions of the Creative Commons Attribution (CC BY) license (<https://creativecommons.org/licenses/by/4.0/>).

## 1. Introduction

The environmental requirements for carbonate emissions are being tightened, and the construction of new alumina refineries processing raw materials by sintering is prohibited, while the existing refineries are subjected to mothballing. These requirements have been implemented in the U.S.A. and Europe and are beginning to take effect in China. Therefore, new plants using hydrometallurgical technologies are being constructed. The proposed hydrometallurgical technologies for alumina production also have disadvantages resulting from overgrowing the heating surfaces of autoclave equipment and the need to use calcium carbonate calcination to obtain calcium oxide. To solve these problems, the use of calcium oxide must be replaced with the use of other compounds available in mineral ores and anthropogenic waste [1].

Aluminosilicates originate from Al<sub>2</sub>O<sub>3</sub>–SiO<sub>2</sub> systems. The introduction of calcium oxide into an Al<sub>2</sub>O<sub>3</sub>–SiO<sub>2</sub> system during leaching of aluminosilicate raw materials replaces Al<sub>2</sub>O<sub>3</sub> with CaO and forms calcium silicate in the aluminate solution [2,3].

Sintering and hydrochemical methods are used to process highly siliceous bauxite.

In the process of bauxite sintering, CaO is added to bind SiO<sub>2</sub> and obtain 2CaO–SiO<sub>2</sub>. The disadvantages of this method are the high capital intensity and energy consumption,

as well as the low stability and the possibility that the  $2\text{CaO-SiO}_2$  will decompose during the processing of the sinter and lead to the loss of alkali and alumina [4].

CaO is not used during the hydrochemical processing of high-modulus bauxite with a silicon modulus exceeding 7, since the  $\text{SiO}_2$  content is low enough, and the losses are insignificant.

In processing highly siliceous bauxites, calcium oxide is added during the leaching of high-modulus alkaline solutions to obtain insoluble calcium silicate compounds without aluminum. With the use of Bayer hydrochemical technology, sodium calcium hydrosilicate  $\text{Na}_2\text{O-CaO-SiO}_2\text{-H}_2\text{O}$  (SCHS) is formed, and with Bayer hydrogarnet technology, the alumina-iron hydrogarnet  $3\text{CaO-Fe}_2\text{O}_3\text{-2SiO}_2\text{-2H}_2\text{O}$  is formed.

The efficiency of hydrochemical technologies depends on the activity of calcium oxide or its derivatives introduced into the alkaline aluminosilicate slurry.

The authors of [5] described a method for the synthesis of calcium oxide by heat treatment of an aqueous solution of calcium acetate and D-glucose at 350 and then at 700 °C. In this case, highly dispersed calcium oxide with an average particle size of 77 nm formed. This technology is intended for low-tonnage production and is not suitable for the production of alumina with a CaO demand of approximately 1 million tons.

For the  $\text{CaO-SiO}_2\text{-H}_2\text{O}$  system, more than 17 phases are known, and their composition depends on the initial  $\text{CaO/SiO}_2$  ratio and on the temperature [6–16]. Unibasic (tobermoritic) and biaxial hydrosilicates are characteristic of alumina production and can be used as fillers during the preparation of composite materials [12–28]. They are formed during the hydrochemical processing of the sinter due to the interactions of the  $2\text{CaO-SiO}_2$  sinter with dilute aluminate solutions as well as from alkali regeneration of sodium-calcium hydrosilicates during leaching with different variants of the Ponomarev-Sazhin method.

In the  $\text{Na}_2\text{O-CaO-SiO}_2\text{-H}_2\text{O}$  system, calcium hydrosilicate and SCHS may be stable phases, depending on the combination of temperature and alkali concentration [10].

The physicochemical properties of NaOH and KOH solutions differ significantly. The electrolyte activity coefficient in NaOH solutions is about an order of magnitude smaller than in potassium solutions, and, consequently, the chemical activity of sodium solutions is lower.

Certain differences in the behavior of individual sodium and potassium compounds are primarily due to the chemical properties of the sodium and potassium ions. The potassium ion has a larger ionic radius than the sodium ion, i.e., 1.33 Å vs. 0.98 Å of the latter. This explains the lower hydration capacity of potassium compared to sodium. Potassium ions weaken the bonds between water molecules in the hydrate shell and promote an increase in the translational movement of water molecules surrounding the ions; sodium ions, on the contrary, reduce the mobility of water molecules near the ions and promote the strengthening of bonds between water molecules.

## 2. Materials and Methods and Results

X-ray fluorescence analysis of the chemical composition of the samples was performed on a Venus 200 wave dispersion spectrometer (Panalytical B. V., Almelo, The Netherlands). Chemical analysis was performed using an Optima 2000 DV inductively coupled plasma optical emission spectrometer (Perkin Elmer, Waltham, MA, USA). Semi-quantitative X-ray phase analysis was performed on a D8 Advance diffractometer (BRUKER, Billerica, MA, USA) using copper (Cu)  $K\alpha$  radiation at an accelerating voltage of 36 kV and a current of 25 mA.

Coarseness was determined with a Winner 2000 laser particle size analyzer of the Photocor series, the measurement principle of which involves static and dynamic light scattering.

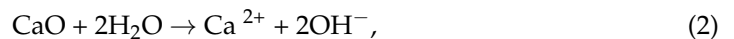
### 2.1. Lime Quenching Mechanism

The mechanism for quenching has not been studied sufficiently, but preference is given for its explanation to the crystallization theory, describing the dissolution of CaO followed by the crystallization of Ca(OH)<sub>2</sub>.

A scheme is proposed for CaO dissolution via the sequential reactions:



It is assumed that in the process of calcium oxide dissolution, supersaturated solutions are obtained due to the formation of complex dihydrates with CaO·2H<sub>2</sub>O composition. The process of calcium oxide hydration by water proceeds according to



followed by the crystallization from the Ca(OH)<sub>2</sub> solution.

Ion hydration leads to the self-dispersion of CaO colloids, which naturally accelerates the solid–phase interactions between CaO and water.

Thus, the overall process of CaO dissolution in water is reduced to the initial hydration of CaO in solution, and the chemical interaction of CaO with water results in the formation of hydrated calcium ions. After saturation of the solution, dissolution of CaO stops, Ca(OH)<sub>2</sub> crystallizes from the solution, and the process of CaO hydration proceeds in solid phase.

The solubility of Ca(OH)<sub>2</sub> in water and in alkaline solutions decreases with increasing temperature. At 90 °C, the solubility in water is 0.591 g/L, at 120 °C, it is 0.40, at 150 °C, it is 0.247, and at 200 °C, it is 0.05 g/L. In alkaline solutions, the solubility is negligible [4]. There are reports indicating that in the presence of silica, the solubility of CaO increases because the sodium silicate solution acts as a liquid ionite, transferring and retaining the calcium ions in solution. As a result of its low solubility, CaO is almost completely incorporated into the crystallizing solid phases. The compositions and structures of these compounds depend on the conditions under which the interactions occur (concentration, ratio of the components and temperature) [12].

The structure of the Ca(OH)<sub>2</sub> powder, including its coarseness as a function of temperature and quenching duration, was investigated.

The effects of the calcium oxide quenching temperature were studied at 20–200 °C (Table 1 and Figures A1–A5).

**Table 1.** Effect of quenching temperature on particle size.

Temperature, °C	Particle Size, nm	Area, %	∑ Particles Less Than 1000 nm
20	14.62	71.1	71.1
	7.9 × 10 <sup>5</sup>	28.9	
130	0.549	3	86.4
	5.406	6.8	
	69.79	56.7	
	1664	19.9	
	4.1 × 10 <sup>5</sup>	13.6	
150	1.848	5.4	89.5
	58.49	18.9	
	3950	65.2	
	1.7 × 10 <sup>4</sup>	10.5	
180	0.957	1.1	93.2
	4.29	5.2	
	64.52	14.8	
	4949	72.1	
	1.4 × 10 <sup>7</sup>	6.9	
200	0.506	0.4	94.7
	4.82	5.1	
	153.6	89.2	
	2.6 × 10 <sup>6</sup>	5.3	

The effect of CaO quenching duration was studied in the 120–1440 min range at a temperature of 130 °C (Table 2 and Figures A6–A10).

**Table 2.** Effect of quenching duration on particle size.

Duration, min	Particle Size, nm	Area, %	$\Sigma$ Particles Less Than 1000 nm
120	0.172	7.1	85.0
	15.61	16	
	86.83	12	
	850.3	49.9	
	$1.7 \times 10^6$	15	
240	1.368	2.5	62.5
	19.73	27.1	
	165.8	32.8	
	5908	37.5	
360	0.355	3.5	55.1
	13.82	23	
	126.3	28.6	
	$1.1 \times 10^4$	36.4	
	$1.1 \times 10^7$	8.5	
480	0.955	6.4	14.3
	45.12	7.8	
	$1.8 \times 10^4$	82.3	
	$2.7 \times 10^7$	3.4	
1440	1.304	10.8	14.1
	42.47	3.2	
	$6.5 \times 10^4$	65.2	
	$8.7 \times 10^7$	20.7	

Thus, an increase in the duration of the quenching process led to increases in the particle size, which reduced the activity of the reagent.

Analyses of the results obtained from a study of the structure of the Ca(OH)<sub>2</sub> powder as a function of temperature and duration of CaO quenching showed that:

- With increasing temperature, the particle size decreased;
- With increasing duration, the particles became larger;
- The optimum conditions for quenching were obtained at a temperature of 200 °C and with a quenching duration of 2 h.

With the existing design of the industrial hardware used for autoclave leaching, it is reasonable to use a temperature of 130 °C, which provides acceptable particle sizes.

## 2.2. Influence of the Calcium Additive in Systems with Participation of Na<sub>2</sub>O

We investigated the behavior of the CaO–Al<sub>2</sub>O<sub>3</sub>–SiO<sub>2</sub> system in sodium alkaline solutions with the calcium-containing materials calcium carbonate CaCO<sub>3</sub>, gypsum CaSO<sub>4</sub>–H<sub>2</sub>O, calcium oxide CaO and calcium hydroxide Ca(OH)<sub>2</sub>.

The clay fraction of kaolinite clay from the Alexeevskoye deposit, which was practically a monophase comprising kaolin Al<sub>2</sub>(Si<sub>2</sub>O<sub>5</sub>)(OH)<sub>4</sub>, was used, the basis of which was the Al<sub>2</sub>O<sub>3</sub>–SiO<sub>2</sub> system.

The chemical composition of the kaolinite clay, in wt. %, was Al<sub>2</sub>O<sub>3</sub>, 35.6; SiO<sub>2</sub>, 43.2; and other components, 21.2; the silicon modulus ( $\mu_{Si}$ ) was 0.6.

The kaolinite clay resembled loose sand with a whitish color; its density was  $2.06 \text{ g/cm}^3$ , its bulk density was  $1.36 \text{ kg/cm}^3$ , its pH was 7.7, and its average grain size was 2 mm.

The  $\text{CaO-Al}_2\text{O}_3\text{-SiO}_2$  system was studied with solutions containing  $240 \text{ g/dm}^3$  of  $\text{Na}_2\text{O}$  with a liquid-to-solid ratio of 10.0, at a temperature of  $240 \text{ }^\circ\text{C}$  and for a duration of 240 min; a thermostat unit was used, with six autoclaves rotating through the head and a working volume of  $250 \text{ cm}^3$  (Figure 1).



Figure 1. Thermostat plant with autoclaves.

The reagents used in the work were chemically pure  $\text{CaCO}_3$ ,  $\text{CaSO}_4$  and  $\text{CaO}$ .  $\text{Ca(OH)}_2$  was obtained by the  $\text{CaO}$  quenching method.

A study of the forms for the calcium-containing additives showed that when using  $\text{CaCO}_3$ , the release of  $\text{Al}_2\text{O}_3$  into the solution did not occur. In the  $\text{CaO-Al}_2\text{O}_3\text{-SiO}_2$  system, phase transformations occurred as follows (Figure 2):

- The calcium-containing phases  $\text{Ca(OH)}_2$  and  $\text{Ca}_4(\text{Si}_6\text{O}_{15})(\text{OH})_2(\text{H}_2\text{O})_5$  were formed;
- When kaolin  $\text{Al}_2\text{O}_3\text{-2SiO}_2\text{-2H}_2\text{O}$  interacted with  $\text{NaOH}$ , sodium hydroaluminosilicates were formed with different compositions;
- A phase comprising sodium silicate and tobermorite was formed.

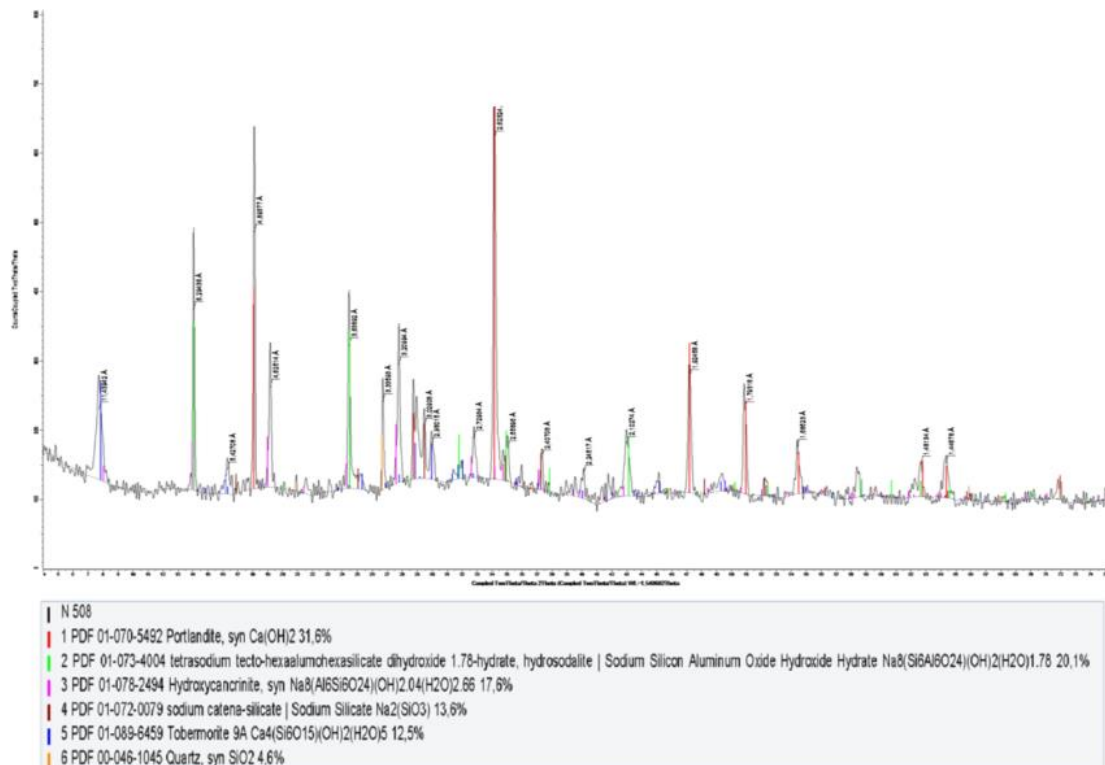
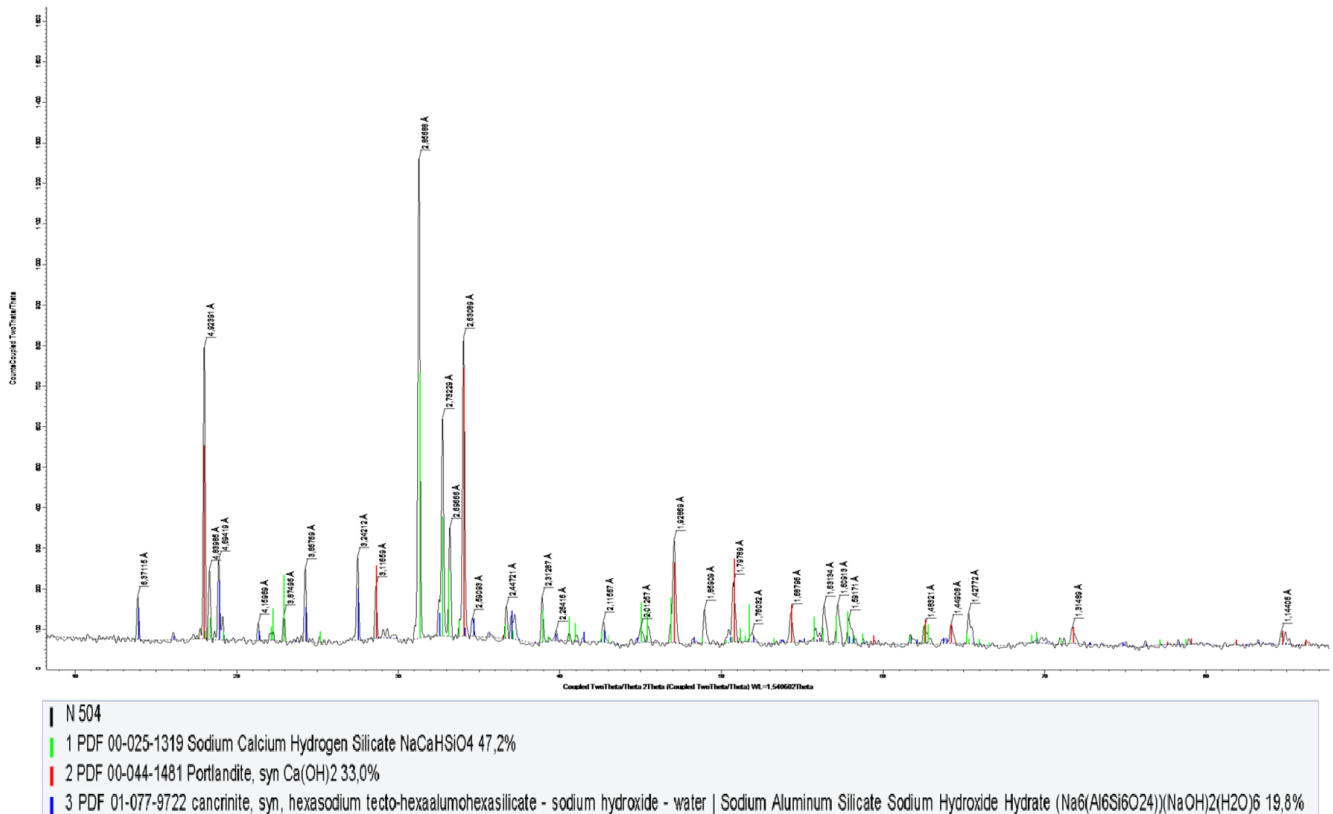


Figure 2. Phase composition of the kaolin leach cake with  $\text{CaCO}_3$  after activation.

When  $\text{CaSO}_4$  was used, no  $\text{Al}_2\text{O}_3$  was released into the solution. Phase transformations did occur in the system as follows (Figure 3):

- The calcium-containing phases  $\text{Ca}(\text{OH})_2$  and  $\text{NaCaHSiO}_4$  were formed;
- When kaolin,  $\text{Al}_2\text{O}_3\text{-}2\text{SiO}_2\text{-}2\text{H}_2\text{O}$ , interacted with  $\text{NaOH}$ , cancrinite,  $(\text{Na}_6(\text{Al}_6\text{Si}_6\text{O}_{24}))(\text{NaOH})_2(\text{H}_2\text{O})_6$ , was formed.



**Figure 3.** Phase composition of the activation cake with  $\text{CaSO}_4$ .

In studies using  $\text{Ca}(\text{OH})_2$ , calcium hydroxide was obtained by quenching calcium oxide at room temperature, with a liquid-to-solid ratio of 3:1. The liquid phase was separated by filtration. The moisture content of the product was 50%.

When using  $\text{Ca}(\text{OH})_2$ , the rate for recovery of  $\text{Al}_2\text{O}_3$  from the alkaline solution was 26.61%.

The phase composition of the obtained cake is shown in Figure 4.

To increase the efficiency of  $\text{Ca}(\text{OH})_2$  utilization, hydrothermal activation of the calcium-containing additives, including  $\text{CaO}$  quenching at  $130\text{ }^\circ\text{C}$ , was investigated.

After high-temperature quenching, the efficiency of  $\text{Al}_2\text{O}_3$  extraction into the solution was increased to 69.34%.

The phase composition of the cake obtained with  $\text{Ca}(\text{OH})_2$  quenched at  $130\text{ }^\circ\text{C}$  is shown in Figure 5.

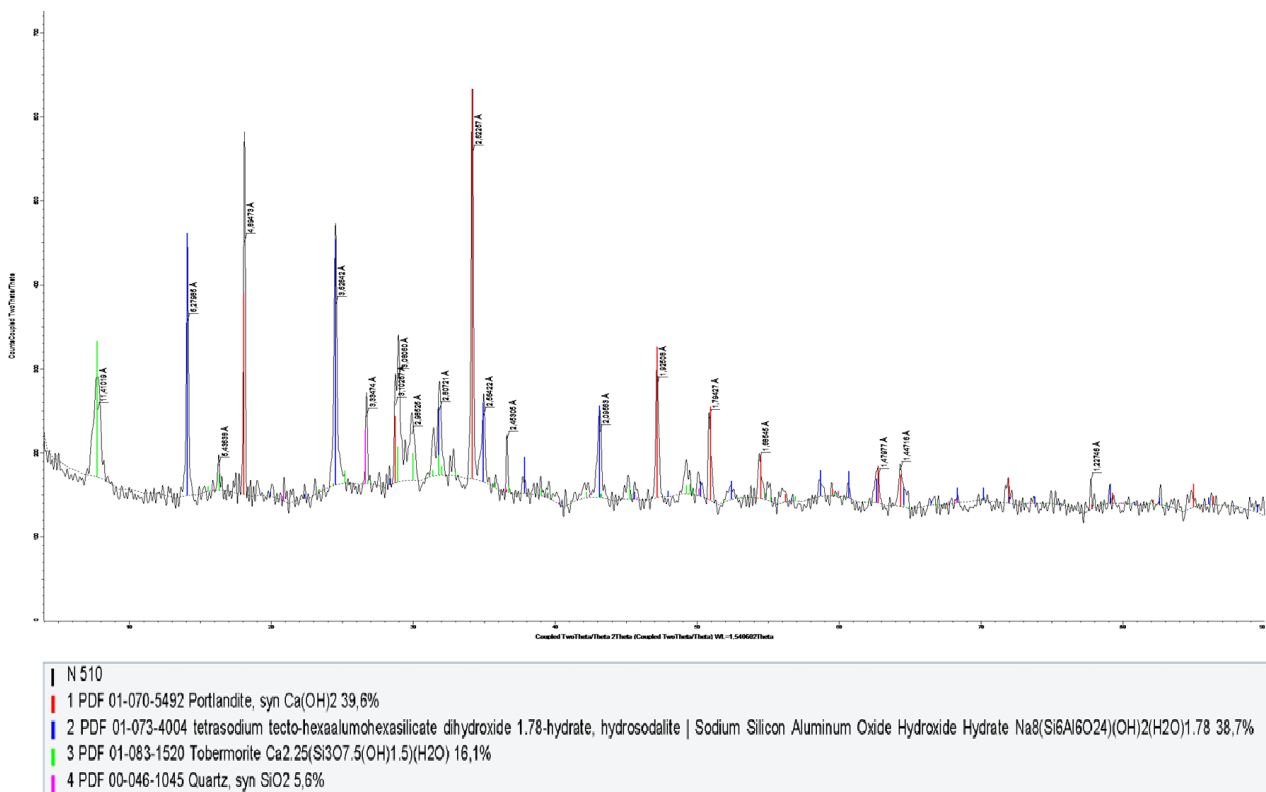


Figure 4. Phase composition of the cake obtained from  $\text{Ca}(\text{OH})_2$  after quenching at 25 °C.

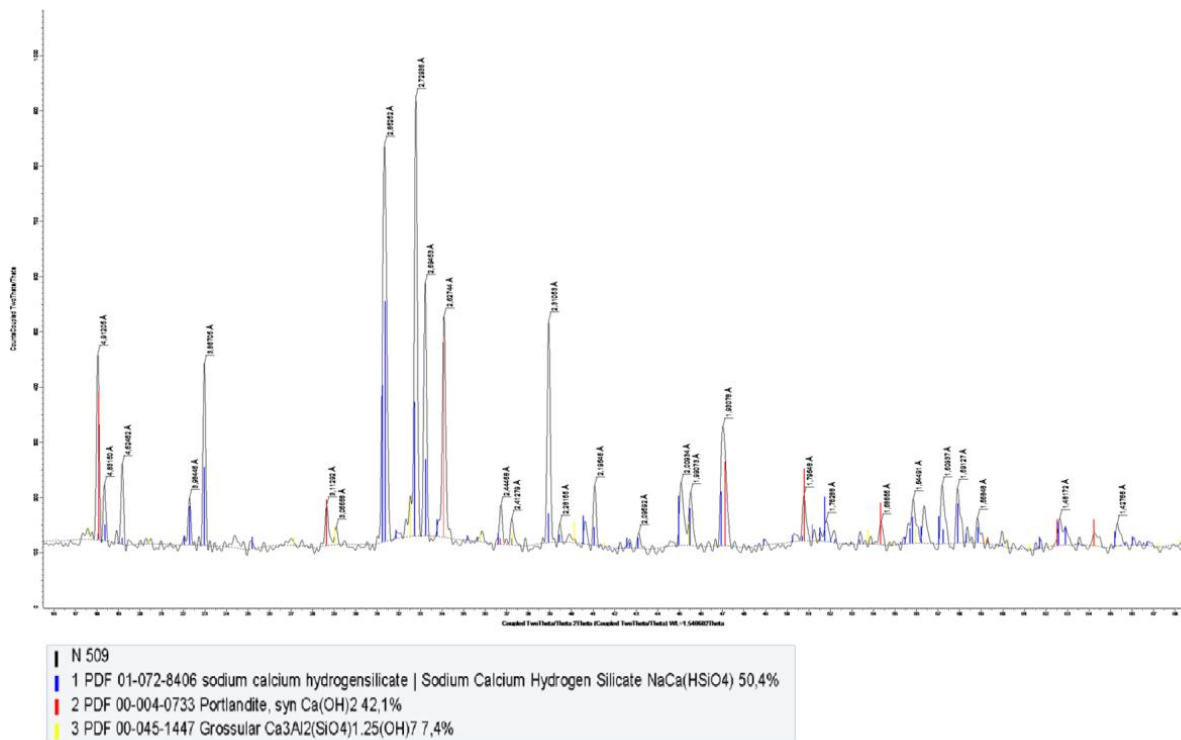


Figure 5. Phase composition of the cake obtained with  $\text{Ca}(\text{OH})_2$  after quenching at 130 °C.

The increased rate of the extraction of  $\text{Al}_2\text{O}_3$  from the solution is explained by the fact that increasing the temperature of CaO quenching increased the activity of the resulting  $\text{Ca}(\text{OH})_2$ . Earlier, it was noted that increasing temperature enhanced the quenching process and improved the quality of the product by increasing the dispersibility of the powder. The productivity of the process increased by a factor of 7–8 in comparison with that obtained with low-temperature quenching (25 °C).

### 2.3. Influence of the Calcium Additive in Systems with Participation of $\text{K}_2\text{O}$

It used to be thought that potassium solutions of alkalis and aluminates behaved in the same way as sodium solutions, but recent studies in this field indicate that their behavior is not always the same. For example, when kaolins are treated with potassium aluminate solutions at a temperature of about 100 °C, the formation of potassium aluminosilicates practically does not occur, while sodium aluminosilicate under the same conditions is formed quickly, completely binding all the silica.

We investigated the behavior of the  $\text{CaO-K}_2\text{O-Al}_2\text{O}_3\text{-SiO}_2$  system in sodium alkaline solutions with the calcium-containing materials calcium carbonate  $\text{CaCO}_3$ , gypsum  $\text{CaSO}_4\text{-H}_2\text{O}$ , calcium oxide  $\text{CaO}$  and calcium hydroxide  $\text{Ca}(\text{OH})_2$ .

The  $\text{CaO-K}_2\text{O-Al}_2\text{O}_3\text{-SiO}_2$  system was studied with solutions containing 240 g/dm<sup>3</sup> of  $\text{K}_2\text{O}$  with a liquid-to-solid ratio of 8.0, at a temperature of 240 °C and for a duration of 240 min.

The replacement of sodium oxide with potassium oxide up to 32–33 did not reduce the degree of extraction of the main components into the solution. A further increase in the proportion of potassium in the initial solution up to 55–56 contributed to a sharp decrease in the content of aluminum and potassium in the solution after leaching. Increasing the amount of  $\text{K}_2\text{O}$  up to 100 negatively affected the process of decomposition of the raw materials, with a further decrease in the degree of transition of aluminum and potassium into the solution.

The chemical composition of the samples depending on the calcium-containing additive used for the activation is presented in Table 3.

**Table 3.** The chemical composition of the samples depending on the calcium-containing additive used for the activation.

Calcium-Containing Additive	Content, %			
	CaO	K <sub>2</sub> O	Al <sub>2</sub> O <sub>3</sub>	SiO <sub>2</sub>
CaO	14.77	10.19	13.1	22.9
CaSO <sub>4</sub>	21.6	12.13	3.9	10.4
Ca(OH) <sub>2</sub>	23.06	0	3.74	20.45
CaCO <sub>3</sub>	10.8	12.77	7.0	15.8

A study of calcium-containing additives showed that when using  $\text{CaCO}_3$ , the rate of recovery of  $\text{Al}_2\text{O}_3$  from the alkaline solution was 47.62%.

In the  $\text{CaO-K}_2\text{O-Al}_2\text{O}_3\text{-SiO}_2$  system, phase transformations occurred as follows (Figure 6):

- When silica interacted with calcium, wollastonite, jaffeite, tobermorite and gahlenite were formed;
- When kaolin  $\text{Al}_2\text{O}_3\text{-2SiO}_2\text{-2H}_2\text{O}$  interacted with KOH, potassium hydroaluminosilicates were formed with different compositions;
- An aluminum silicate hydroxide phase was formed.

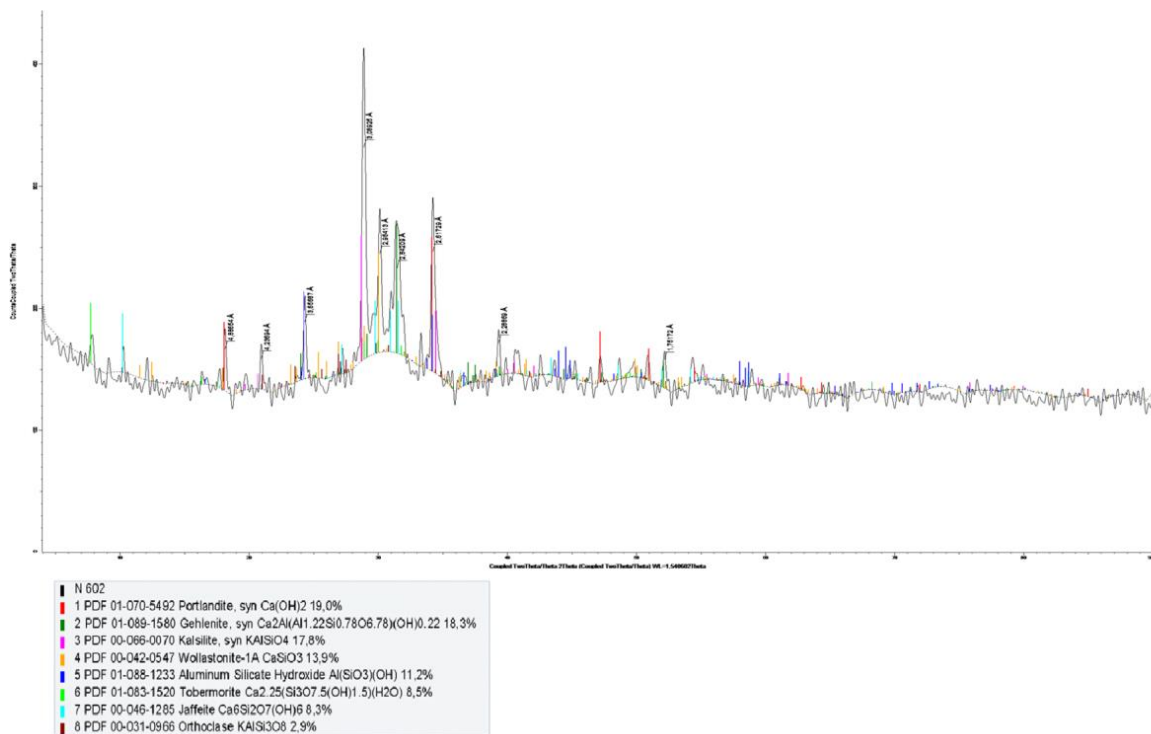


Figure 6. Phase composition of the kaolin leach cake with CaCO<sub>3</sub> after activation.

When CaSO<sub>4</sub> was used, the rate of recovery of Al<sub>2</sub>O<sub>3</sub> from the alkaline solution was 63.83%. Phase transformations did occur in the system as follows (Figure 7):

- When silica interacted with calcium, jaffeite was formed;
- When kaolin Al<sub>2</sub>O<sub>3</sub>-2SiO<sub>2</sub>-2H<sub>2</sub>O interacted with KOH, potassium aluminosilicates were formed with different compositions.

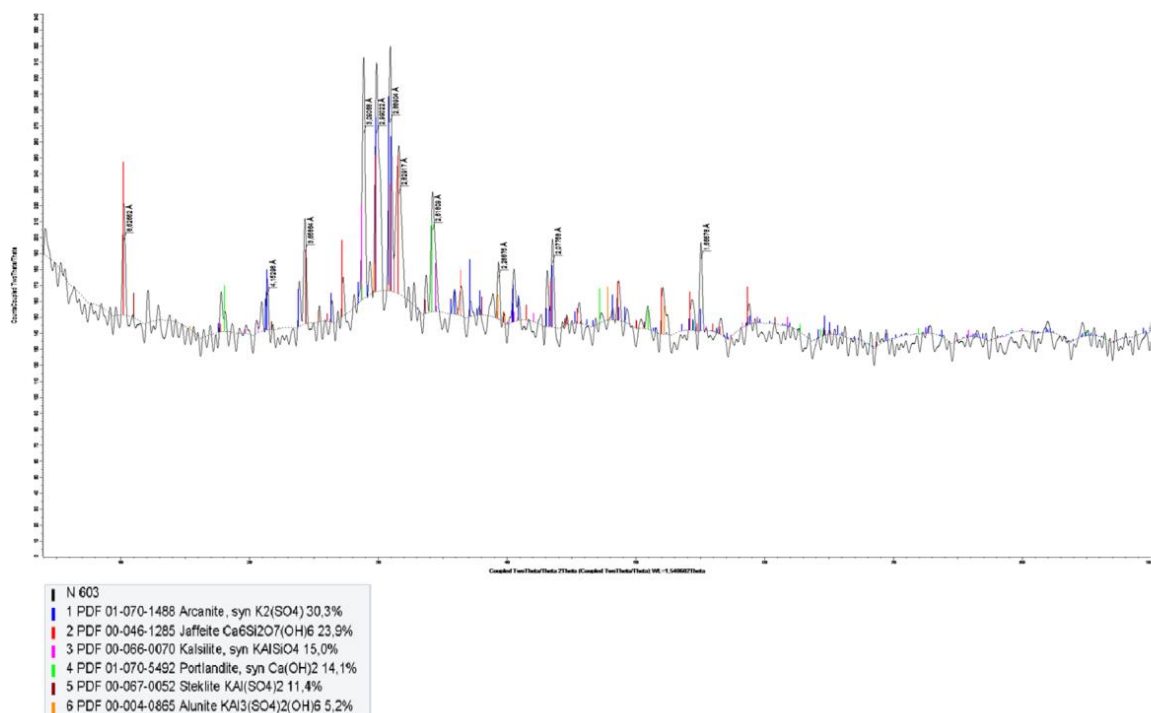
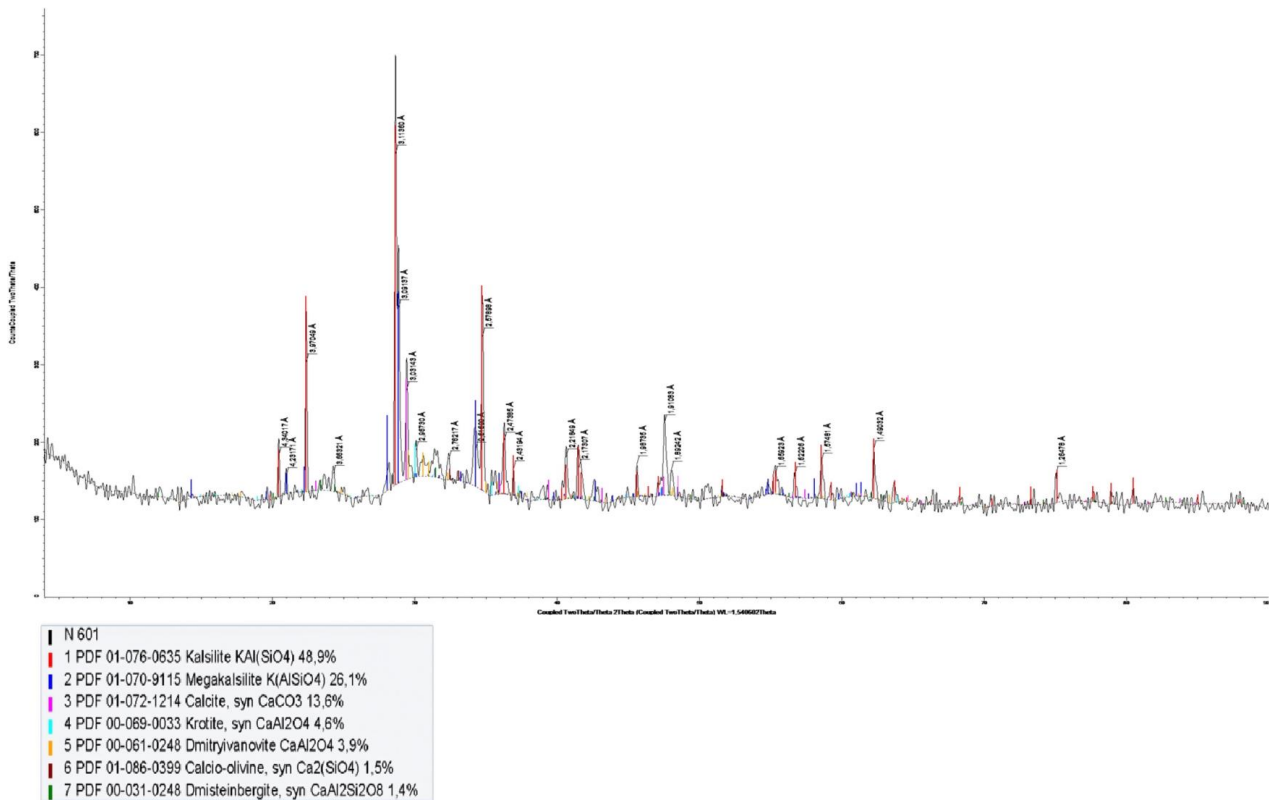


Figure 7. Phase composition of the kaolin leach cake with CaSO<sub>4</sub>.

When CaO was used, the rate of recovery of  $\text{Al}_2\text{O}_3$  from the alkaline solution was 42.6%. Phase transformations did occur in the system as follows (Figure 8):

- When silica interacted with calcium, calcio-olivine and dmisteinbergite were formed;
- When kaolin  $\text{Al}_2\text{O}_3\text{-2SiO}_2\text{-2H}_2\text{O}$  interacted with KOH, potassium aluminosilicates were formed with different compositions.



**Figure 8.** Phase composition of the kaolin leach cake with CaO.

In studies using  $\text{Ca}(\text{OH})_2$  quenching at room temperature, the rate of recovery of  $\text{Al}_2\text{O}_3$  from the alkaline solution was 11.87%. Phase transformations did occur in the system as follows (Figure 9):

- Aluminum interacted with potassium and silicon to form megakalsite;
- A portlandite phase and reinhardbraunsite were formed.

In studies using  $\text{Ca}(\text{OH})_2$  quenching at 130 °C, the rate of recovery of  $\text{Al}_2\text{O}_3$  from the alkaline solution was 12.51%. Phase transformations did occur in the system as follows (Figure 10):

- Aluminum interacted with potassium and silicon to form kaliophilite;
- A portlandite phase and dellaite and calcite were formed.

The effect of calcium additives to sodium and potassium alkali during kaolin leaching on the degree of  $\text{Al}_2\text{O}_3$  extraction is presented in Table 4.

The study showed that when leaching in sodium alkali, the highest aluminum recovery was achieved using  $\text{Ca}(\text{OH})_2$  quenched at 130 °C, while when leaching in potassium alkali, the highest aluminum recovery was achieved using calcium sulfate.

The obtained alkali aluminate solutions were processed by crystallization.

The process of crystalline precipitation from solution consists of four stages: formation of a supersaturated solution, formation of crystal nuclei, i.e., crystallization centers, crystal growth, and crystallization itself.



**Table 4.** The effect of calcium additives to sodium and potassium alkali during kaolin leaching on the degree of Al<sub>2</sub>O<sub>3</sub> extraction.

Calcium-Containing Additive	NaOH	KOH
CaCO <sub>3</sub>	0	47.62
CaSO <sub>4</sub>	0	63.83
Ca(OH) <sub>2</sub> , quenching at 25 °C.	26.61	11.87
Ca(OH) <sub>2</sub> , quenching at 130 °C.	69.34	12.51

The rate of crystal growth depends on the process conditions. To form nuclei, supersaturation of the solution was carried out by evaporation. Then, the supersaturated solution was cooled to promote the spontaneous growth of a new nucleate phase.

Recrystallization was carried out by removing the residual supersaturation of the solution and recrystallizing the precipitate.

The solubility in the K<sub>2</sub>O–Al<sub>2</sub>O<sub>3</sub>–H<sub>2</sub>O system at 30, 60 and 90 °C was investigated (Tables 5–7).

**Table 5.** Solubility in the system K<sub>2</sub>O–Al<sub>2</sub>O<sub>3</sub>–H<sub>2</sub>O at 30 °C.

Equilibrium Solution Composition, g/dm <sup>3</sup>				Sediment Composition, %				Note
K <sub>2</sub> O	Al <sub>2</sub> O <sub>3</sub>	H <sub>2</sub> O	α <sub>k</sub>	K <sub>2</sub> O	Al <sub>2</sub> O <sub>3</sub>	H <sub>2</sub> O	α <sub>k</sub>	
9.5	0.9	89.6	10.0	3.5	31.4	65.1	0.12	The precipitate is insoluble
15.1	1.8	83.1	9.1	6.1	36.3	57.6	0.18	The precipitate is insoluble
19.2	3.0	77.8	7.0	8.2	42.2	49.6	0.21	The precipitate is insoluble
23.0	4.5	72.5	5.6	15.1	33.7	51.2	0.49	The precipitate is insoluble
28.3	15.2	56.5	2.0	21.3	25.2	53.5	0.92	The precipitate is insoluble
29.5	16.9	53.6	1.9	-	-	-	-	The precipitate is partially soluble
32.0	10.1	57.9	3.4	34.1	28.4	37.5	1.31	The precipitate is soluble
34.3	5.8	59.9	6.4	37.0	18.2	44.8	2.21	The precipitate is soluble
38.2	3.1	58.7	13.4	38.2	25.1	36.7	1.65	The precipitate is soluble
42.5	1.5	56.0	30.7	41.1	12.1	46.8	3.69	The precipitate is soluble
44.5	1.05	54.45	46.0	44.4	8.7	46.9	5.52	The precipitate is soluble

**Table 6.** Solubility in the K<sub>2</sub>O–Al<sub>2</sub>O<sub>3</sub>–H<sub>2</sub>O system at 60 °C.

Equilibrium Solution Composition, g/dm <sup>3</sup>				Sediment Composition, %				Note
K <sub>2</sub> O	Al <sub>2</sub> O <sub>3</sub>	H <sub>2</sub> O	α <sub>k</sub>	K <sub>2</sub> O	Al <sub>2</sub> O <sub>3</sub>	H <sub>2</sub> O	α <sub>k</sub>	
10.0	3.1	86.9	3.52	6.5	21.1	72.3	0.33	The precipitate is insoluble
11.2	4.2	84.5	2.9	6.8	29.3	63.9	0.25	The precipitate is insoluble
13.1	5.1	81.8	2.8	11.1	20.0	68.9	0.6	The precipitate is insoluble
19.0	8.8	79.2	2.3	13.5	28.9	57.6	0.51	The precipitate is insoluble
24.2	15.5	60.3	1.7	9.8	42.0	48.2	0.25	The precipitate is insoluble
27.2	19.8	53.0	1.5	19.7	31.1	49.2	0.69	The precipitate is insoluble
28.2	21.1	50.8	1.5	-	-	-	-	The precipitate is partially soluble
35.1	10.2	54.7	3.7	33.4	21.2	45.4	1.71	The precipitate is soluble
40.3	4.3	55.4	10.0	38.2	14.5	47.3	2.86	The precipitate is soluble
42.5	3.1	54.4	14.9	42.1	19.5	38.4	2.34	The precipitate is soluble
45.3	2.2	52.5	22.4	32.1	26.2	41.7	1.33	The precipitate is soluble

**Table 7.** Solubility in the  $K_2O-Al_2O_3-H_2O$  system at 90 °C.

Equilibrium Solution Composition, g/dm <sup>3</sup>			$\alpha_k$	Sediment Composition, %			$\alpha_k$	Note
K <sub>2</sub> O	Al <sub>2</sub> O <sub>3</sub>	H <sub>2</sub> O		K <sub>2</sub> O	Al <sub>2</sub> O <sub>3</sub>	H <sub>2</sub> O		
8.5	4.6	86.9	2.0	4.0	32.3	63.7	0.13	The precipitate is insoluble
13.6	7.8	78.6	1.9	11.5	24.6	63.9	0.51	The precipitate is insoluble
15.5	9.2	75.3	1.8	13.8	23.2	63.0	0.64	The precipitate is insoluble
18.0	12.2	69.8	1.6	10.4	34.5	55.1	0.33	The precipitate is insoluble
23.5	18.8	57.7	1.4	10.2	40.3	50.5	0.27	The precipitate is insoluble
26.6	22.8	50.6	1.3	20.2	34.2	45.8	0.63	The precipitate is insoluble
28.1	25.8	46.1	1.2	-	-	-	-	The precipitate is partially soluble
31.8	19.0	49.2	1.8	33.2	28.8	38.8	1.25	The precipitate is soluble
34.5	14.9	56.6	2.5	38.0	33.1	28.9	1.24	The precipitate is soluble
37.5	11.0	51.5	3.7	39.2	23.3	97.5	1.82	The precipitate is soluble
42.1	6.2	51.7	7.4	40.9	27.5	31.6	1.61	The precipitate is soluble

The analysis of the solubility showed that with the increase in  $K_2O$  concentration from 9.5–29.5% the equilibrium concentration of  $Al_2O_3$  increased, and the caustic ratio decreased accordingly.

At a  $K_2O$  content in the solution up to 18%, the equilibrium concentration of  $Al_2O_3$  increased slowly from 0.9%  $Al_2O_3$  (with 9.5%  $K_2O$ ) to 3%  $Al_2O_3$  (with 19.2%  $K_2O$ ). With a further increase in caustic alkali concentration, a decrease in the  $Al_2O_3$  equilibrium concentration was observed, and the  $Al_2O_3$  equilibrium concentration curve sloped steeply downward. Accordingly, a sharp increase in the caustic ratio occurred at  $K_2O$  contents up to 38%. At increases in alkali concentration above 38%, the curve descended.

The unsaturated solution regions increased with increasing temperature and, correspondingly, the supersaturated solution regions decreased.

The caustic ratios of equilibrium solutions in the  $K_2O-Al_2O_3-H_2O$  system are shown in Figure 11.

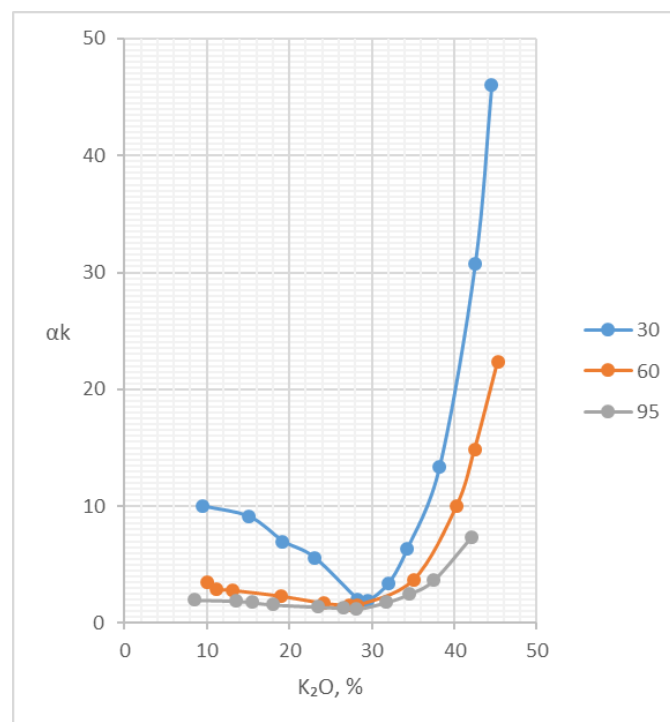


**Figure 11.** Caustic ratios of equilibrium solutions in the  $K_2O-Al_2O_3-H_2O$  system.

According to Figure 11, the caustic ratios of equilibrium solutions in the system gradually decreased with increasing  $K_2O$  concentration up to 29.5 at 30 °C, being 1.89 at 28.1  $K_2O$  at 60 °C, 1.44 at 28.1  $K_2O$  at 95 °C and finally reaching the lowest value of 1.18. With further increase in  $K_2O$  concentration, we observed a sharp increase in  $\alpha_k$ , which was due to the conversion of the solid hydroxide phase to aluminate and its precipitation from the solution.

The caustic ratios of the precipitates depended on the degree of squeezing and on the concentration of the alkali in the equilibrium solutions. The isotherms of the  $Na_2O-Al_2O_3-H_2O$  and  $K_2O-Al_2O_3-H_2O$  systems at 30° are similar in appearance, while at 60 and 95 °C, they differ markedly. The branches of the latter system at 60 and 95 °C are steeper than those of the first system.

The composition of the solid phase of both systems in the left branches of the curves is the same, i.e., gibbsite, while in the right branches, the solid phases differ not only by the nature of the alkali in the composition of the aluminates, but also by the amount of alkali and crystallization water.

While in the  $Na_2O-Al_2O_3-H_2O$  system the aluminates  $Na_2O-Al_2O_3-2.5 H_2O$  and  $3Na_2O-Al_2O_3-6 H_2O$  were formed, in the  $K_2O-Al_2O_3-H_2O$  system, only  $K_2O-Al_2O_3-3H_2O$  precipitated at concentrations of  $K_2O$  up to 45.

In the  $K_2O-Al_2O_3-H_2O$  system, the equilibrium of the solutions was established in a shorter time than in the  $Na_2O-Al_2O_3-H_2O$  system.

This study showed that when leaching in sodium alkali, the highest aluminum recovery was achieved using  $Ca(OH)_2$  quenched at 130 °C, while when leaching in potassium alkali, the highest aluminum recovery was achieved using calcium sulfate.

### 3. Conclusions

The behavior of the  $CaO-Al_2O_3-SiO_2$  system was investigated in alkaline solution with calcium-containing materials including calcium carbonate  $CaCO_3$ , gypsum  $CaSO_4-H_2O$ , calcium oxide  $CaO$  and calcium hydroxide  $Ca(OH)_2$ .  $Ca(OH)_2$  was obtained with the  $CaO$  quenching method. The extraction of  $Al_2O_3$  in the alkaline solution was only possible with the use of  $Ca(OH)_2$ , and the efficiency of the extraction depended on the conditions of  $CaO$  quenching.

The structure of the  $Ca(OH)_2$  powder and its coarseness as a function of the temperature and duration of the quenching were investigated.

The analysis of the structure of the  $Ca(OH)_2$  powder as a function of the temperature and duration of  $CaO$  quenching showed the following:

- With increasing temperature, the particle size decreased;
- With increasing duration, the particles became larger;
- The optimal parameters for obtaining a fine powder were a temperature of 200 °C and a duration of 2 h.

**Author Contributions:** Conceptualization, R.A.; methodology, N.A., S.G. and O.K.; investigation, N.A., S.G. and O.K.; data curation, N.A., N.S. and O.K.; writing—original draft preparation, R.A.; writing—review and editing, S.G.; visualization, N.A., O.K. and O.M.; project administration, R.A. All authors have read and agreed to the published version of the manuscript.

**Funding:** This research was funded by the Science Committee of the Ministry of Science and Higher Education of the Republic of Kazakhstan, Grant number BR18574018.

**Data Availability Statement:** The data used to support the findings of this study are included within the article.

**Conflicts of Interest:** The authors declare no conflict of interest.

### Appendix A

The effect of  $CaO$  quenching temperature over the range of 20–200 °C is presented in Figures A1–A5.

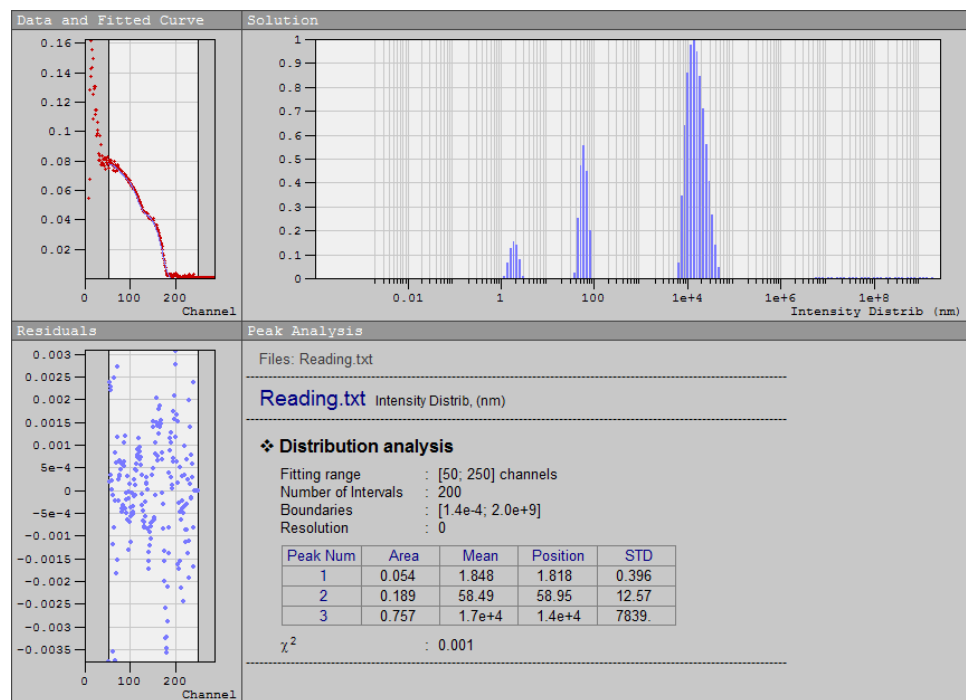


Figure A1. Structure of the Ca(OH)<sub>2</sub> powder quenched at 20 °C for 2 h.

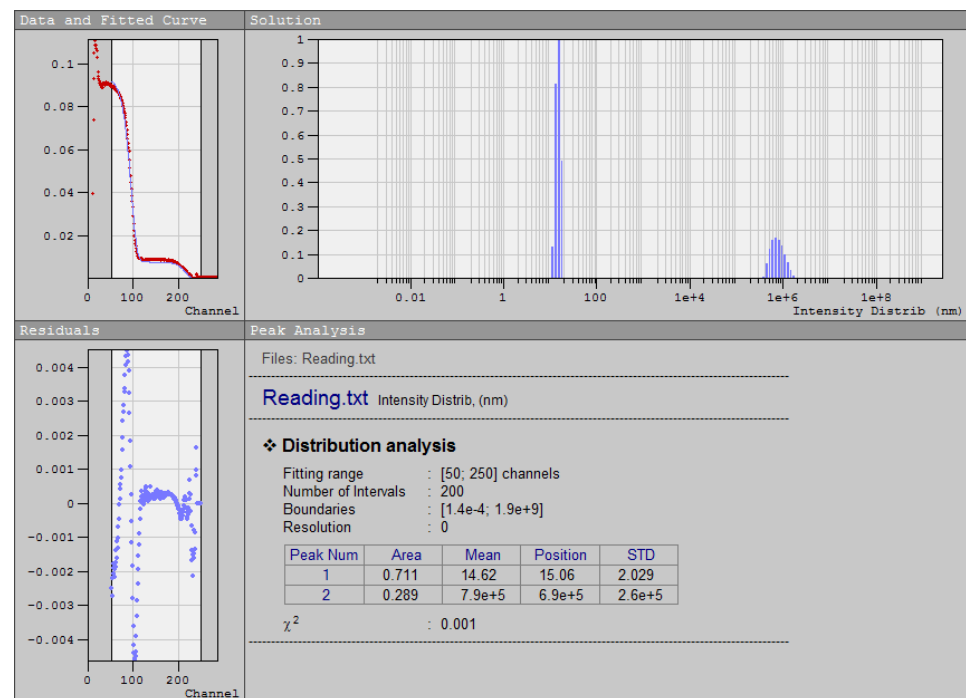


Figure A2. Structure of the Ca(OH)<sub>2</sub> powder quenched at 130 °C for 2 h.

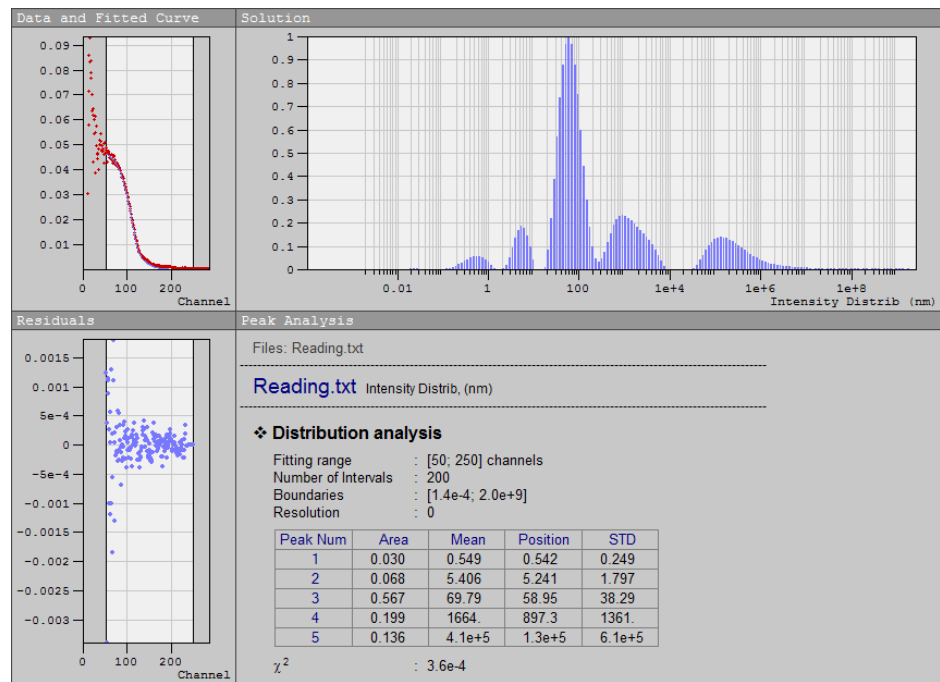


Figure A3. Structure of the  $\text{Ca}(\text{OH})_2$  powder quenched at 150 °C for 2 h.

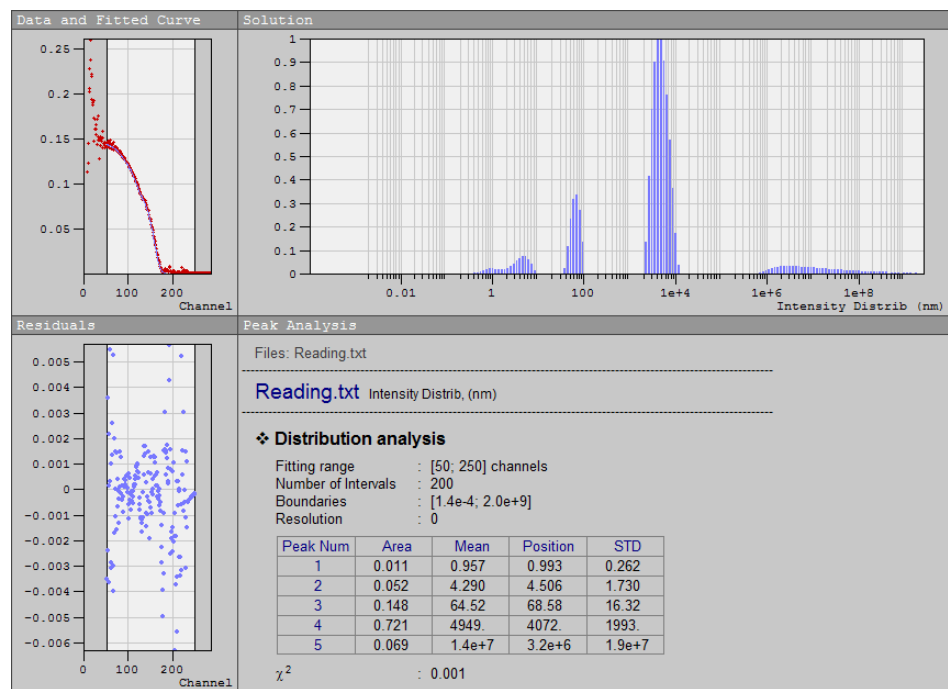


Figure A4. Structure of the  $\text{Ca}(\text{OH})_2$  powder quenched at 180 °C for 2 h.

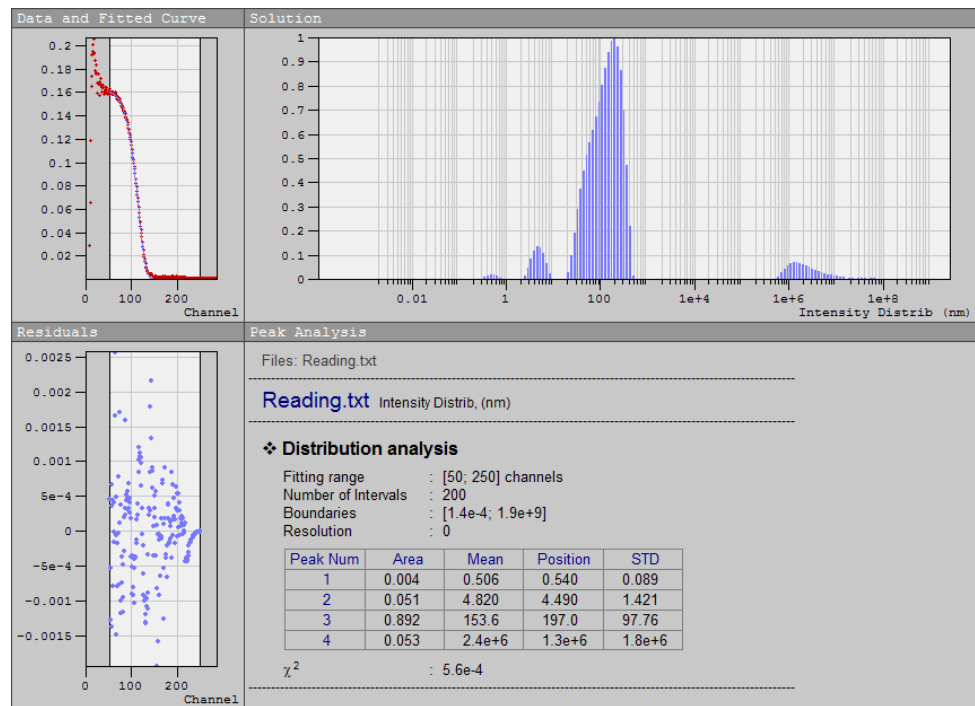


Figure A5. Structure of the Ca(OH)<sub>2</sub> powder quenched at 200 °C for 2 h.

### Appendix B

The effect of CaO quenching duration over the range of 120–1440 min t a temperature of 130 °C is presented in Figures A6–A10.

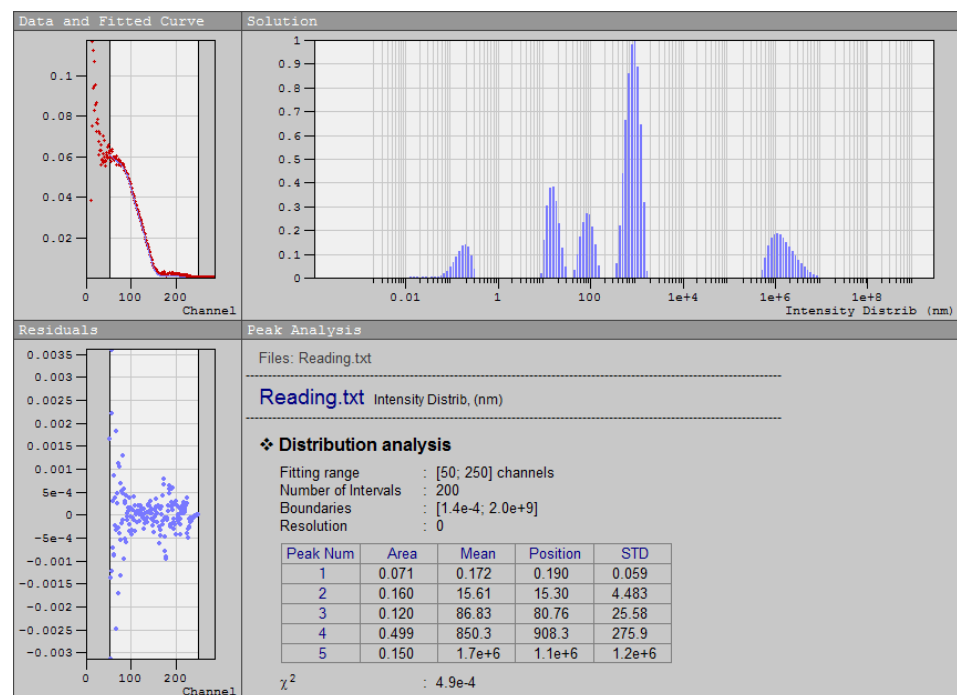


Figure A6. Structure of the CaO powder quenched at 130° for 2 h.

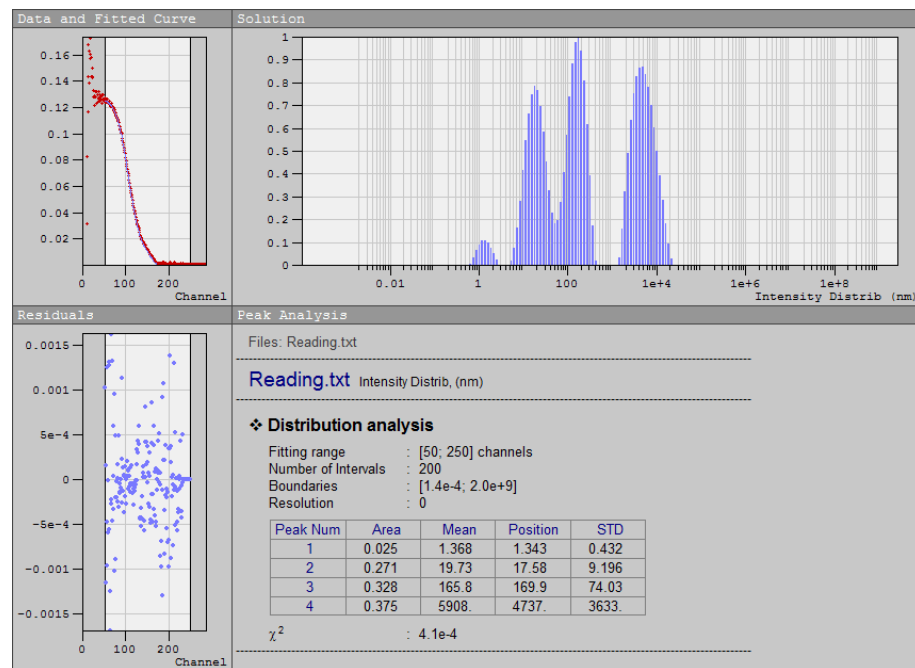


Figure A7. Structure of the CaO powder quenched at 130° for 4 h.

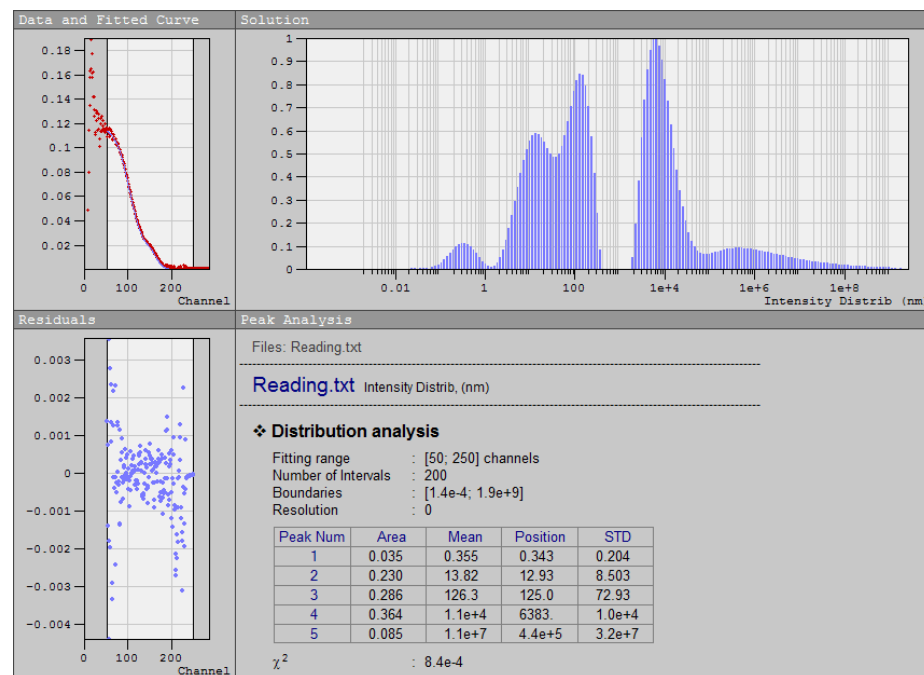


Figure A8. Structure of the CaO powder quenched at 130° for 6 h.

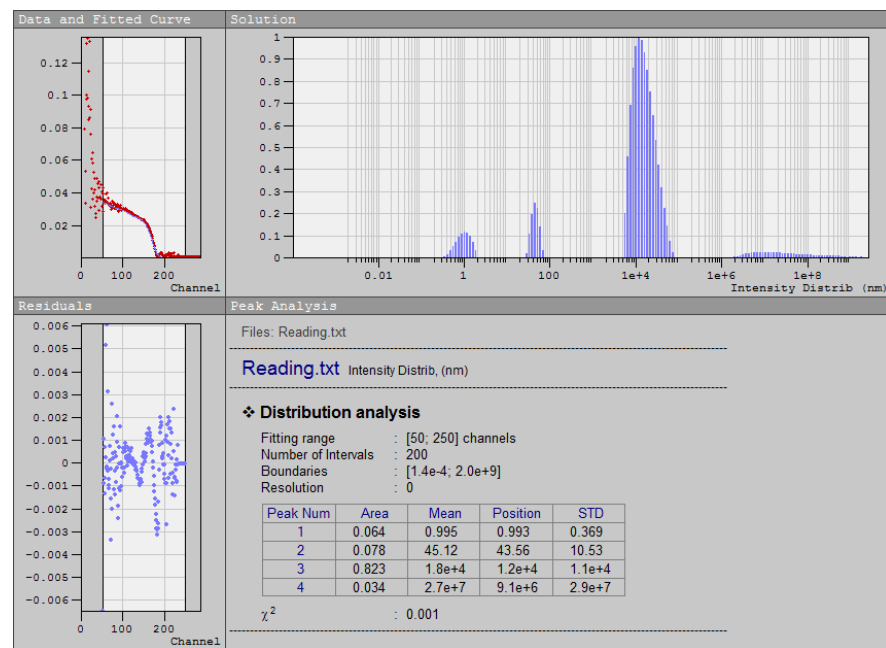


Figure A9. Structure of the CaO powder quenched at 130° for 8 h.

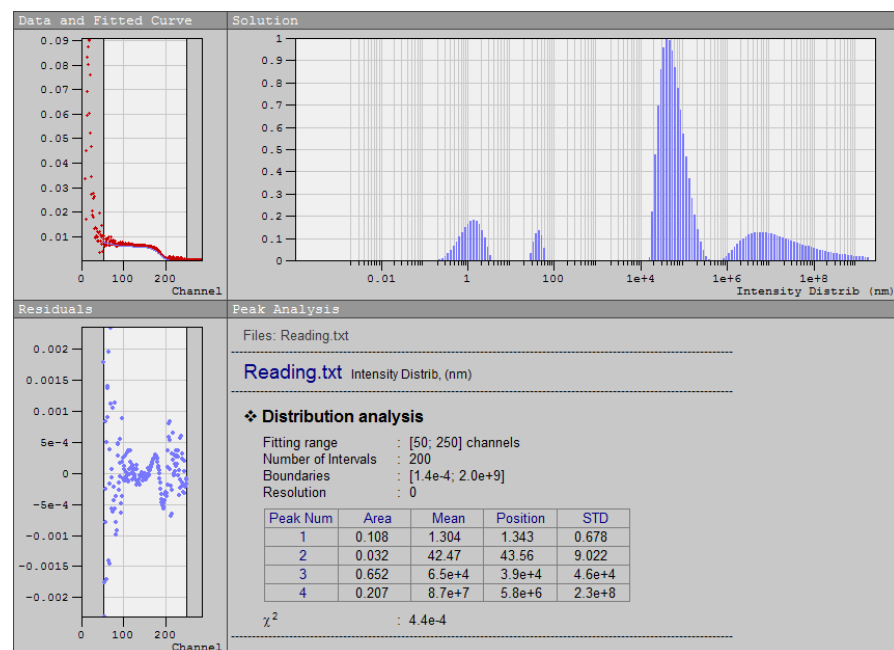


Figure A10. Structure of CaO powder quenched at 130° for 24 h.

## References

1. Global Alumina Market Analysis 2018–2022, Forecast 2023–2027. Businessstat. 2023. Available online: <https://www.businessresearchinsights.com/market-reports/alumina-market-109644> (accessed on 16 March 2023).
2. Ibragimov, A.T.; Budon, S.V. *Development of Technology of Alumina Production from Bauxites of Kazakhstan*; Pavlodar, Kazakhstan, 2010; pp. 8–10.
3. Ni, L.P.; Raizman, V.L.; Khalyapina, O.B. *Production of Alumina*; Reference ed.; Institute of Metallurgy and Enrichment NAS: Almaty, Kazakhstan, 1998; 356p.
4. Ni, L.P.; Khalyapina, O.B. *Physico—Chemical Properties of Raw Materials and Products of Alumina Production*; Science: Almaty, Kazakhstan, 1978; 118p.
5. Kozerozhets, I.V.; Panasyuk, G.P.; Semenov, E.A.; Voroshilov, I.L.; Avdeeva, V.V.; Buzanov, G.A.; Danchevskaya, M.N.; Kolmakova, A.A.; Malinina, E.A. A new approach to the synthesis of nanosized powder CaO and its application as precursor for the synthesis of calcium borates. *Ceram. Int.* **2022**, *48*, 7522–7532. [CrossRef]

6. Nekhoroshev, E. Thermodynamic Optimisation of the  $\text{Na}_2\text{O-K}_2\text{O-Al}_2\text{O}_3\text{-CaO-MgO-B}_2\text{O}_3\text{-SiO}_2$  System. Ph.D. Thesis, Polytechnique Montréal, Montreal, QC, Canada, 2019. PolyPublie. Available online: <https://publications.polymtl.ca/4133/> (accessed on 19 April 2023).
7. Li, M.; Utigard, T.; Barati, M. Kinetics of  $\text{Na}_2\text{O}$  and  $\text{B}_2\text{O}_3$  Loss From  $\text{CaO-SiO}_2\text{-Al}_2\text{O}_3$  Slags. *Metall. Mater. Trans. B* **2015**, *46*, 74–82. [[CrossRef](#)]
8. Schairer, J.F.; Yoder, H.S., Jr. *The Quaternary System  $\text{Na}_2\text{O-MgO-Al}_2\text{O}_3\text{-Al}_2\text{O}_3\text{-SiO}_2$* ; Year Book—Carnegie Institution: Washington, DC, USA, 1958; pp. 210–213.
9. Jung, I.-H.; Decterov, S.A.; Pelton, A.D. Critical Thermodynamic Evaluation and Optimisation of the  $\text{MgO-Al}_2\text{O}_3$ ,  $\text{CaO-MgO-Al}_2\text{O}_3$  and  $\text{MgO-Al}_2\text{O}_3\text{-SiO}_2$  Systems. *J. Phase Equilib.* **2004**, *25*, 329–345. [[CrossRef](#)]
10. Chen, M.; Xinmei, H.; Junhong, C.; Baojun, Z. Phase Equilibria Studies in the  $\text{SiO}_2\text{-K}_2\text{O-CaO}$  System. *Metall. Mater. Trans. B* **2016**, *47*, 1690–1696. [[CrossRef](#)]
11. Zhang, Z.; Xiao, Y.; Voncken, J.H.L.; Yang, Y.; Boom, R.; Wang, N.; Zou, Z. Phase equilibria in the  $\text{Na}_2\text{O-CaO-SiO}_2$  system. *J. Am. Ceram. Soc.* **2011**, *94*, 3088–3093. [[CrossRef](#)]
12. Klyuev, S.V.; Klyuev, A.V.; Khezhev, T.A.; Pukhareno, Y.V. Technogenic Sands as Effective Filler for Fine-Grained Fibre Concrete. *J. Phys. Conf. Ser.* **2018**, *1118*, 012020. [[CrossRef](#)]
13. Khudiyakova, T.M.; Kolesnikov, A.S.; Zhakipbaev, B.E.; Kenzhibaeva, G.S.; Kutzhanova, A.N.; Iztleuov, G.M.; Zhanikulov, N.N.; Kolesnikova, O.G.; Mynbaeva, E. Optimization of Raw Material Mixes in Studying Mixed Cements and Their Physicomechanical Properties. *Refract. Ind. Ceram.* **2019**, *60*, 76–78. [[CrossRef](#)]
14. Kolesnikova, O.; Vasilyeva, N.; Kolesnikov, A.; Zolkin, A. Optimization of raw mix using technogenic waste to produce cement clinker. *MIAB Min. Inf. Anal. Bull.* **2022**, *60*, 103–115. [[CrossRef](#)]
15. Zhanabay, N.; Suleimenov, U.; Utebayeva, A.; Kolesnikov, A.; Baibolov, K.; Imanaliyev, K.; Moldagaliyev, A.; Karshyga, G.; Duissenbekov, B.; Fediuk, R.; et al. Analysis of a Stress-Strain State of a Cylindrical Tank Wall Vertical Field Joint Zone. *Buildings* **2022**, *12*, 1445. [[CrossRef](#)]
16. Zharmenov, A.; Yefremova, S.; Satbaev, B.; Shalabaev, N.; Satbaev, S.; Yermishin, S.; Kablanbekov, A. Production of Refractory Materials Using a Renewable Source of Silicon Dioxide. *Minerals* **2022**, *12*, 1010. [[CrossRef](#)]
17. Ostrowski, C.; Zelazny, J. Solid solutions of calcium aluminates C3A, C12A7 and CA with sodium oxide. *J. Therm. Anal. Calorim.* **2004**, *75*, 867–885. [[CrossRef](#)]
18. Kolesnikov, A.S. Thermodynamic simulation of silicon and iron reduction and zinc and lead distillation in zincoligonite ore-carbon systems. *Russ. J. Non-Ferrous Metals* **2014**, *55*, 513–518. [[CrossRef](#)]
19. Mamyrbekova, A.; Mamitova, A.D.; Mamyrbekova, A. Electrochemical Behavior of Sulfur in Aqueous Alkaline Solutions. *Russ. J. Phys. Chem. A* **2018**, *92*, 582–586. [[CrossRef](#)]
20. Satbaev, B.; Yefremova, S.; Zharmenov, A.; Kablanbekov, A.; Yermishin, S.; Shalabaev, N.; Satbaev, A.; Khen, V. Rice Husk Research: From Environmental Pollutant to a Promising Source of Organo-Mineral Raw Materials. *Materials* **2021**, *14*, 4119. [[CrossRef](#)] [[PubMed](#)]
21. Kolesnikov, A.S.; Sapargaliyeva, B.O.; Bychkov, A.Y.; Alferyeva, Y.O.; Syrlybekkyzy, S.; Altybaeva, Z.K.; Nurshakhanova, L.K.; Seidaliyeva, L.K.; Suleimenova, B.S.; Zhidebayeva, A.E.; et al. THERMODYNAMIC MODELING OF THE FORMATION OF THE MAIN MINERALS OF CEMENT CLINKER AND ZINC FUMES IN THE PROCESSING OF TOXIC TECHNOGENIC WASTE OF THE METALLURGICAL INDUSTRY. *Ras. J. Chem.* **2022**, *15*, 2181–2187. [[CrossRef](#)]
22. Muratov, B.; Kolesnikov, A.; Shapalov, S.; Syrlybekkyzy, S.; Volokitina, I.; Zhunisbekova, D.; Takibayeva, G.; Nurbaeva, F.; Aubakirova, T.; Nurshakhanova, L.; et al. Physico-Chemical Study of the Possibility of Utilization of Coal Ash by Processing as Secondary Raw Materials to Obtain a Composite Cement Clinker. *J. Compos. Sci.* **2023**, *7*, 234. [[CrossRef](#)]
23. Kolesnikov, A.S.; Zhanikulov, N.N.; Syrlybekkyzy, S.; Kolesnikova, O.G.; Shal, A.L. Utilization of Waste from the Enrichment of Non-Ferrous Metal Ores as Secondary Mineral Raw Materials in the Production of Cement Clinker. *Ecol. Ind. Russ.* **2023**, *27*, 19–23. [[CrossRef](#)]
24. Ivanushkin, M.A.; Abovyan, P.R.; Butakov, B.I.; Gorovoy, P.I.; Streltsov, M.V.; Tereshchenko, Y.V. Method of Lime Quenching and Lime Quencher for Its Implementation. Patent RU 2285675 C2, 20 October 2006.
25. Mwase, J.M.; Safarian, J. Desilication of Sodium Aluminate Solutions from the Alkaline Leaching of Calcium-Aluminate Slags. *Processes* **2022**, *10*, 1769. [[CrossRef](#)]
26. Yang, Z.; Zhang, D.; Jiao, Y.; Fang, C.; Kang, D.; Yan, C.; Zhang, J. Crystal Evolution of Calcium Silicate Minerals Synthesized by Calcium Silicon Slag and Silica Fume with Increase of Hydrothermal Synthesis Temperature. *Materials* **2022**, *15*, 1620. [[CrossRef](#)]
27. Xie, Z.; Jiang, T.; Chen, F.; Guo, Y.; Wang, S.; Yang, L. Phase Transformation and Zinc Extraction from Zinc Ferrite by Calcium Roasting and Ammonia Leaching Process. *Crystals* **2022**, *12*, 641. [[CrossRef](#)]
28. Sugita, H.; Oguma, T.; Hara, J.; Zhang, M.; Kawabe, Y. Effects of Silicic Acid on Leaching Behavior of Arsenic from Spent Calcium-Based Adsorbents with Arsenite. *Sustainability* **2021**, *13*, 12937. [[CrossRef](#)]

**Disclaimer/Publisher’s Note:** The statements, opinions and data contained in all publications are solely those of the individual author(s) and contributor(s) and not of MDPI and/or the editor(s). MDPI and/or the editor(s) disclaim responsibility for any injury to people or property resulting from any ideas, methods, instructions or products referred to in the content.